Mon. Not. R. Astron. Soc. **276**, 283–292 (1995)

Helioseismic estimation of convective overshoot in the Sun

Jørgen Christensen-Dalsgaard,[1] Mário J.P.F.G. Monteiro[2,3,4] and Michael J. Thompson[2]

[1] *Teoretisk Astrofysik Center, Danmarks Grundforskningsfond, and Institut for Fysik og Astronomi, Aarhus Universitet, DK-8000 Aarhus C, Denmark*

[2] *Astronomy Unit, School of Mathematical Sciences, Queen Mary & Westfield College, Mile End Road, London E1 4NS*

[3] *Grupo de Matemática Aplicada da Faculdade de Ciências, Universidade do Porto, Rua das Taipas 135, 4000 Porto, Portugal*

[4] *Centro de Astrofísica da Universidade do Porto, Rua do Campo Alegre 823, 4100 Porto, Portugal*

Accepted 1995 April 13. Received 1995 April 13; in original form 1994 December 20

ABSTRACT

By using the periodic signal present in the frequencies of oscillation due to the base of the solar convection zone, Monteiro, Christensen-Dalsgaard & Thompson gave an upper limit to the extent of a layer of convective overshooting in the Sun. Alternative studies have suggested that it may not be possible to do so since the amplitude of the signal does not vary monotonically with the extent of the layer.

In this work a new more complete set of models is used to compare the values of the amplitude obtained from the fitting of the signal with the expected amplitudes. These are determined using the assumption that the rapid variation occurring at the base of the convection zone and creating the periodic signal can be described as discontinuities of the sound-speed derivatives. The amplitude of the signal due to the discontinuity of the third derivative of the sound speed is then proportional to the derivative of the radiative gradient, while the amplitude resulting from the discontinuity of the second derivative is proportional to the difference between radiative and adiabatic gradients at the position where the transition occurs. The latter is non-zero only if overshoot is present.

Asymptotic predictions of the amplitudes of the signal in the p-mode frequencies are in good agreement with the values found from fitting models with substantial overshoot regions; as was also found by Monteiro et al., the observed solar frequencies place severe limits on the extent of overshoot of this nature.

Key words: convection – Sun: interior – Sun: oscillations.

1 INTRODUCTION

A localized or sharp feature in the Sun's internal structure will give rise to a characteristic periodic signal in the frequencies of global p modes. Such a sharp feature occurs in standard solar models at the base of the outer convective envelope. An even sharper transition occurs in models incorporating an overshoot layer beneath the convection zone. Monteiro, Christensen-Dalsgaard & Thompson (1994; henceforth MCDT) calibrated the amplitude of the signal in the frequencies with the extent ℓ_s of the overshoot region. The calibration was then used with the solar data to give an upper limit on ℓ_s. Similar results were obtained by Basu, Antia & Narasimha (1994). However, an alternative study (Roxburgh & Vorontsov 1994; in the following RV) has suggested that this scaling should be used carefully since the amplitude is not a monotonically varying function of ℓ_s. As one increases ℓ_s from zero (no overshoot) the amplitude first decreases, before ultimately increasing with more extensive overshoot layers. Such behaviour could restrict the limit that can be imposed on the extent of overshoot from this type of analysis.

In this paper, we extend the analysis of MCDT to determine the dependence of the amplitude on ℓ_s. We start by relating the derivatives of the sound speed to the derivatives of the temperature gradient. Then, approximating the functional behaviour of the gradient by a function involving a step function and the radiative and adiabatic gradients, terms involving the Dirac δ function and its derivative are isolated in the derivatives of the sound speed. Such terms, when used in the variational analysis of MCDT, provide the expression for the amplitude of the signal.

A sequence of models with increasing overshoot distance is then considered, to compare the values obtained by fitting the signal in the frequencies of such models and the expected values given by the analysis. We extend the fitting procedure presented by MCDT, in order to include the dependence of the amplitude on the degree of the modes; we find that the inferred extent of overshoot depends little on this effect. We then consider the expression given by RV and compare it with the values obtained in this work. Finally we discuss the impact upon the earlier published limits on the extent of overshoot in the Sun.

2 SOUND SPEED AND THE TEMPERATURE GRADIENT

Simple descriptions of overshoot (e.g. Zahn 1991) are typically expressed in terms of the behaviour of the temperature gradient $\nabla \equiv \mathrm{d}\log T/\mathrm{d}\log p$, where T is the temperature and p the pressure. However, the effects of sharp features on p-mode frequencies are most naturally expressed in terms of second and third derivatives of the squared sound speed

$$c^2 = \frac{\Gamma_1 p}{\rho}\,, \tag{1}$$

where ρ is density and $\Gamma_1 = (\partial \ln p/\partial \ln \rho)_s$ is the adiabatic exponent, the derivative being at constant specific entropy s. Here we analyse these derivatives in terms of derivatives of ∇, using as independent variable the acoustic depth τ, related to the radius r through $\mathrm{d}r = -c\mathrm{d}\tau$, with τ being equal to zero at the surface of the model. The details of the analysis are presented in Appendix A.

We assume that at the base of the convective envelope the gas is fully ionized and that the composition is constant. Then, e.g., $\mathrm{d}\Gamma_1/\mathrm{d}\tau = 0$, and the expressions for the derivatives are greatly simplified. From equation (1) we find that the first, second and third derivatives of c^2 can be expressed as

$$\frac{\mathrm{d}c^2}{\mathrm{d}\tau} = d_{10} + d_{11}\,\frac{\nabla-\nabla_a}{\nabla_a}\,, \tag{2}$$

$$\begin{aligned}\frac{\mathrm{d}^2c^2}{\mathrm{d}\tau^2} =& d_{20} + d_{21}\left(\frac{\nabla-\nabla_a}{\nabla_a}\right) + d_{22}\left(\frac{\nabla-\nabla_a}{\nabla_a}\right)^2 \\ &+ d_{23}\,\frac{\mathrm{d}}{\mathrm{d}\tau}\left(\frac{\nabla-\nabla_a}{\nabla_a}\right)\,,\end{aligned} \tag{3}$$

and

$$\begin{aligned}\frac{\mathrm{d}^3c^2}{\mathrm{d}\tau^3} =& d_{30} + d_{31}\left(\frac{\nabla-\nabla_a}{\nabla_a}\right) + d_{32}\left(\frac{\nabla-\nabla_a}{\nabla_a}\right)^2 \\ &+ d_{33}\,\frac{\mathrm{d}}{\mathrm{d}\tau}\left(\frac{\nabla-\nabla_a}{\nabla_a}\right) + d_{34}\,\frac{\mathrm{d}}{\mathrm{d}\tau}\left(\frac{\nabla-\nabla_a}{\nabla_a}\right)^2 \\ &+ d_{35}\,\frac{\mathrm{d}^2}{\mathrm{d}\tau^2}\left(\frac{\nabla-\nabla_a}{\nabla_a}\right)\,.\end{aligned} \tag{4}$$

Here $\nabla_a = (\partial \log T/\partial \log p)_s$ and the coefficients d_{ij} are continuous functions of the local stratification and are given in Appendix A.

In determining the behaviour of the gradient ∇ with acoustic depth at the base of the convection zone, we shall assume that the transition from adiabatic stratification to radiative stratification occurs over a length scale much shorter than the wavelength of the modes. This fundamental assumption allows us to treat the transition at the base of the convection zone as discontinuities of the sound-speed derivatives. Furthermore, it is assumed that a possible overshoot layer is adiabatically stratified, with a jump to radiative stratification at its boundary. Effects of relaxing these assumptions are discussed in Section 6 below.

We start by writing

$$\nabla-\nabla_a = (\nabla_r-\nabla_a)\,f(\tau)\,, \tag{5}$$

where ∇_r is the radiative gradient (cf. equation 6). Also, we let τ_c be the acoustical depth of the transition from instability to stability according to the Schwarzschild condition (i.e., $\nabla=\nabla_a=\nabla_r$ at $\tau=\tau_c$), whereas the depth at the edge of the overshoot region is denoted τ_d. If we restrict ourselves to the region around the base of the convection zone, the behaviour of the function f is then given by

$$f(\tau) \simeq \begin{cases} 0^+ & ;\ \tau<\tau_c \quad \text{Convection zone} \\ 0 & ;\ \tau=\tau_c \quad \text{Schwarzschild point} \\ 0^+ & ;\ \tau_c<\tau<\tau_d \quad \text{Overshooting} \\ 1 & ;\ \tau\geqslant\tau_d \quad \text{Radiative interior}\,. \end{cases} \tag{6}$$

The value of 0^+ in both the convection zone and the overshoot region reflects the fact that the value of ∇ near the base but inside the convection zone is slightly superadiabatic, while in the overshoot region ($\tau_c<\tau<\tau_d$) the stratification is slightly subadiabatic. If there is no overshoot layer, $\tau_d=\tau_c$.

Neglecting the small departures from adiabatic stratification on either side, to a very good approximation we may write

$$f(\tau) = H(\tau-\tau_d) \equiv \begin{cases} 0 & ;\ \tau<\tau_d \\ 1 & ;\ \tau\geqslant\tau_d\,, \end{cases} \tag{7}$$

where H is the Heaviside (or step) function. Substitution of this expression in equation (5) gives

$$\nabla-\nabla_a = (\nabla_r-\nabla_a)\ H(\tau-\tau_d)\ ; \tag{8}$$

and differentiating it we obtain

$$\frac{\mathrm{d}}{\mathrm{d}\tau}(\nabla-\nabla_a) = (\nabla_r-\nabla_a)\,\delta(\tau-\tau_d) + \frac{\mathrm{d}\nabla_r}{\mathrm{d}\tau}\,H(\tau-\tau_d)\,. \tag{9}$$

Further,

$$\begin{aligned}\frac{\mathrm{d}^2}{\mathrm{d}\tau^2}(\nabla-\nabla_a) =& \ (\nabla_r-\nabla_a)\,\delta'(\tau-\tau_d) \\ &+ 2\,\frac{\mathrm{d}\nabla_r}{\mathrm{d}\tau}\ \delta(\tau-\tau_d) + \frac{\mathrm{d}^2\nabla_r}{\mathrm{d}\tau^2}\,H(\tau-\tau_d)\,,\end{aligned} \tag{10}$$

where δ' is the derivative of the δ function. Note that, in the case of no overshooting, $\nabla_r=\nabla_a$ at $\tau=\tau_c=\tau_d$; hence the terms in $\nabla_r-\nabla_a$ vanish.

We can now write the derivatives of the sound speed as combinations of two parts: one that contains the continuous terms and terms with step functions, denoted by the subscript '$_s$'; and a second which contains δ functions or derivatives thereof. As shown below, only the latter part contributes to the oscillatory signal. From expressions (2) and (8) we obtain

$$\frac{\mathrm{d}c^2}{\mathrm{d}\tau} = \left[\frac{\mathrm{d}c^2}{\mathrm{d}\tau}\right]_s\ ; \tag{11}$$

furthermore, from equations (3), (8) and (9), and using the explicit expression for d_{23}, we have

$$\frac{\mathrm{d}^2c^2}{\mathrm{d}\tau^2} = \left[\frac{\mathrm{d}^2c^2}{\mathrm{d}\tau^2}\right]_s + gc(\gamma-1)\,\frac{\nabla_r-\nabla_a}{\nabla_a}\,\delta(\tau-\tau_d)\,, \tag{12}$$

where g is the gravitational acceleration and $\gamma = c_p/c_V$ is the ratio between the specific heats at constant pressure and constant volume.

In the case with no overshoot, the term in the δ function is zero. Here the oscillatory signal in the frequencies arises from the third derivative of sound speed. This is obtained

from equations (4) and (8) – (10) as

$$\frac{d^3c^2}{d\tau^3} = \left[\frac{d^3c^2}{d\tau^3}\right]_s + \frac{2gc(\gamma-1)}{\nabla_a}\,\delta(\tau-\tau_d) \times\left[\frac{d\nabla_r}{d\tau} - (\nabla_r-\nabla_a)\,\frac{d}{d\tau}\log\left(\frac{c^3}{g^2}\right)\right] + \frac{gc(\gamma-1)}{\nabla_a}\,(\nabla_r-\nabla_a)\,\delta'(\tau-\tau_d)\,. \tag{13}$$

If there is no overshoot we have only the contribution from $d\nabla_r/d\tau$.

3 AMPLITUDE OF THE SIGNAL

We shall now consider the determination, by means of a variational principle, of the amplitude of the signal in the p-mode frequencies due to discontinuities in the derivatives of the sound speed. The analysis is based on expressions given by MCDT; however, rather than treating separately the case without overshoot (as did MCDT), we include throughout the contribution from the third derivative of the sound speed.

The sharp feature at the base of the convection zone or overshoot layer is characterized by the departure δc^2 in the squared sound speed from an assumed 'smooth' model, indicated by the subscript '$_0$'. This model has, by definition, no discontinuous derivatives of any thermodynamic quantity (in particular the sound speed), and hence has no δ function in any derivative of c_0^2. The periodic signal is given (see Appendix B) by

$$\delta\omega \sim \frac{1}{16\omega^2\tau_t}\int_{\tau_a}^{\tau_b}\left\{\left[\frac{1-2\Delta}{1-\Delta}-\Delta_c\right]\frac{d^3}{d\tau^3}\left(\frac{\delta c^2}{c_0^2}\right) - \left[\frac{6\Delta(1+2\Delta)}{(1-\Delta)^2}\,\frac{d}{d\tau}\log\left(\frac{c_0}{r_0}\right)\right]\frac{d^2}{d\tau^2}\left(\frac{\delta c^2}{c_0^2}\right)\right\} \times\frac{\sin(\Lambda)}{(1-\Delta)^{3/2}}\,d\tau\,, \tag{14}$$

where τ_t is the acoustic radius of the Sun and ω is the mode frequency, the interval of integration $[\tau_a,\tau_b]$ in expression (14) being defined such that δc^2 and its derivatives are zero outside it. Here

$$\Delta = \frac{l(l+1)\,c_0^2}{\omega^2 r_0^2}\,, \tag{15}$$

and

$$\Delta_c = \frac{g_0}{\omega^2 c_0}\,\frac{d}{d\tau}\log\left(\frac{g_0}{r_0^2}\right)\,. \tag{16}$$

The effect of the small quantity Δ, which depends on the mode degree l, is negligible for most of the modes considered here, as discussed by MCDT. However, we shall include the dominant terms in Δ in our fit to the frequencies, to demonstrate that its effect is indeed small.

The argument of the sine function is

$$\Lambda = 2\omega\int_0^\tau (1-\Delta)^{1/2}d\tau' + 2\phi\,, \tag{17}$$

where ϕ is the phase.

The next step is to keep track explicitly only of those terms in the second and third derivatives of the sound-speed difference that involve a δ function or its derivative. Noting that from the third derivative of the sound-speed difference there are two such terms (from the second and third derivatives of c^2) and from the second derivative there is one, it can be shown that (using equations (12) and (13))

$$\begin{aligned}\frac{d^2}{d\tau^2}\left(\frac{\delta c^2}{c_0^2}\right) &= \left[\frac{d^2}{d\tau^2}\left(\frac{\delta c^2}{c_0^2}\right)\right]_s + \frac{g_0(\gamma_0-1)}{c_0\,\nabla_{a0}}\,\delta(\tau-\tau_d)(\nabla_{r0}-\nabla_{a0})\,,\\ \frac{d^3}{d\tau^3}\left(\frac{\delta c^2}{c_0^2}\right) &= \left[\frac{d^3}{d\tau^3}\left(\frac{\delta c^2}{c_0^2}\right)\right]_s + \frac{g_0(\gamma_0-1)}{c_0\,\nabla_{a0}}\,\delta(\tau-\tau_d) \times\left[2\frac{d\nabla_{r0}}{d\tau} - (\nabla_{r0}-\nabla_{a0})\,\frac{d}{d\tau}\log\left(\frac{c_0^3}{g_0^2}\right)\right] + \frac{g_0(\gamma_0-1)}{c_0\,\nabla_{a0}}\,\delta'(\tau-\tau_d)\,(\nabla_{r0}-\nabla_{a0})\,.\end{aligned} \tag{18}$$

Substituting in equation (14), the contributions from the δ functions and their derivatives give

$$\begin{aligned}\delta\omega \sim{}& \frac{g_0(\gamma_0-1)}{16\omega^2\tau_t c_0\nabla_{a0}}\,\frac{\sin(\Lambda)}{(1-\Delta)^{3/2}}\left\{\frac{d\nabla_{r0}}{d\tau}\left(\frac{1-2\Delta}{1-\Delta}-\Delta_c\right)\right.\\ &-(\nabla_{r0}-\nabla_{a0})\left[\frac{1-2\Delta}{1-\Delta}\,\frac{d}{d\tau}\log\left(\frac{c_0^2}{g_0}\right)\right.\\ &\left.\left.+\frac{\Delta(7-6\Delta)}{(1-\Delta)^2}\,\frac{d}{d\tau}\log\left(\frac{c_0}{r_0}\right)\right]\right\}\\ &-\frac{g_0(\gamma_0-1)}{8\omega\tau_t c_0\nabla_{a0}}\,\frac{\cos(\Lambda)}{1-\Delta}\,(\nabla_{r0}-\nabla_{a0})\left(\frac{1-2\Delta}{1-\Delta}-\Delta_c\right)\,.\end{aligned} \tag{19}$$

More succinctly, introducing coefficients a_1 and a_2,

$$\delta\omega \sim \frac{1-2\Delta}{(1-\Delta)^2}\left[\frac{a_1}{(1-\Delta)^{1/2}}\left(\frac{\tilde\omega}{\omega}\right)^2\sin(\Lambda) + a_2\left(\frac{\tilde\omega}{\omega}\right)\cos(\Lambda)\right]\,, \tag{20}$$

where $\tilde\omega$ is a reference frequency. This is the expression given by MCDT. However, here we are interested in the actual expressions for a_1 and a_2 and so we have considered higher-order terms in the analysis, obtaining more complete expressions for the coefficients. These are

$$\begin{aligned}a_1 = \frac{g_0(\gamma_0-1)}{16\tilde\omega^2\tau_t c_0\nabla_{a0}}&\left\{\frac{d\nabla_{r0}}{d\tau}\left[1-\frac{\Delta_c(1-2\Delta)}{1-\Delta}\right]\right.\\ &+(\nabla_{r0}-\nabla_{a0})\left[(1-\Delta_c)\,\frac{2c_0}{r_0}\,h(\tau_d)\right.\\ &\left.\left.-\frac{\Delta(7-6\Delta)}{(1-2\Delta)(1-\Delta)}\,\frac{d}{d\tau}\log\left(\frac{c_0}{r_0}\right)\right]\right\},\\ a_2 = -\frac{g_0(\gamma_0-1)}{8\tilde\omega\tau_t c_0\nabla_{a0}}&\,(\nabla_{r0}-\nabla_{a0})\left[1-\frac{\Delta_c(1-2\Delta)}{1-\Delta}\right]\,,\end{aligned} \tag{21}$$

where the function $h(\tau)$ is

$$h(\tau) = \frac{1}{1-\Delta_c}\left[1-\frac{4\pi G r_0\rho_0}{2g_0}-\frac{r_0 g_0}{2c_0^2}\,(\Gamma_{10}-1) -\frac{r_0 g_0}{2c_0^2}\,(\gamma_0-1)\,\frac{\nabla_{r0}-\nabla_{a0}}{\nabla_{a0}}\right]\,, \tag{22}$$

G being the gravitational constant. To the order of the analysis we can consider the values of Δ_c and Δ to be evaluated at $\omega=\tilde{\omega}$. Then a_1 and a_2 are independent of frequency. Also, given that Δ, Δ_c and $\Delta\,\mathrm{d}\log(c_0/r_0)/\mathrm{d}\tau$ are of higher order in small quantities than is Δ_c, we may neglect the terms in a_1 and a_2 that depend on the degree. Therefore, both expressions are also independent of l. The signal is then simply

$$\delta\omega \sim A(\omega,\Delta)\,\cos(\bar{\Lambda})\,, \tag{23}$$

with

$$A(\omega,\Delta)=\frac{1-2\Delta}{(1-\Delta)^2}\left[\frac{a_1^2(\tilde{\omega})}{1-\Delta}\left(\frac{\tilde{\omega}}{\omega}\right)^4+a_2^2(\tilde{\omega})\left(\frac{\tilde{\omega}}{\omega}\right)^2\right]^{1/2} \tag{24}$$

(cf. equation 25). Note that this expression differs from the one given by MCDT in the way in which the contributions from a_1 and a_2 are combined to form $A(\omega,\Delta)$. However, since terms in ω^{-3} were already neglected when deriving this equation (see Appendix B), the actual value for the total amplitude $A(\omega,\Delta)$ is unlikely to depend much on the precise form of the expression. Nevertheless, the values for the individual contributions a_i obtained from fitting to data will differ; thus to compare with equation (31a) obtained by RV we shall use expression (24).

Following MCDT, we write the argument of the signal as

$$\bar{\Lambda}=2\omega\bar{\tau}_\mathrm{d}-\bar{\gamma}_\mathrm{d}\,\frac{l(l+1)}{\omega}+2\phi_0\,, \tag{25}$$

with

$$\begin{aligned}\bar{\tau}_\mathrm{d}&=\tau_\mathrm{d}+a_\phi\,,\\ \bar{\gamma}_\mathrm{d}&=\int_0^{\tau_\mathrm{d}}\frac{\mathrm{d}\tau}{r^2}\;+a_\gamma\,.\end{aligned} \tag{26}$$

The two constants (a_ϕ,a_γ) are corrections due to surface effects. We also introduce a reference degree $\tilde{l}$. The final expression is therefore

$$\begin{aligned}\delta\omega=\frac{1-2\Delta}{(1-\Delta)^2}&\left[\frac{a_1^2}{1-\Delta}\left(\frac{\tilde{\omega}}{\omega}\right)^4+a_2^2\left(\frac{\tilde{\omega}}{\omega}\right)^2\right]^{1/2}\\ &\times\cos\left[2\omega\bar{\tau}_\mathrm{d}-\bar{\gamma}_\mathrm{d}\,\frac{l(l+1)}{\omega}+2\phi_0\right]\,,\end{aligned} \tag{27}$$

where

$$\Delta=\frac{l(l+1)}{\tilde{l}(\tilde{l}+1)}\left(\frac{\tilde{\omega}}{\omega}\right)^2\Delta_\mathrm{d}\,. \tag{28}$$

This is fitted to the data to determine the fitting parameters $(a_1,a_2,\bar{\tau}_\mathrm{d},\bar{\gamma}_\mathrm{d},\phi_0,\Delta_\mathrm{d})$, as described in appendix C of MCDT. In the results presented here we chose the reference values $\tilde{l}=20$ and $\tilde{\omega}/2\pi=2500$ μHz.

4 COMPONENTS OF THE AMPLITUDE

We have two terms contributing to the amplitude of the signal. One, a_1, is associated with the discontinuity of the third derivative of the sound speed and is always present whether there is overshoot or not. However, the other, a_2, is only different from zero if $\tau_\mathrm{d}\neq\tau_\mathrm{c}$, and therefore it only contributes when there is overshoot. Dropping the subscript '$_0$' from all quantities (remembering that they are evaluated at $\tau=\tau_\mathrm{d}$) we find that

$$\begin{aligned}a_1&=\frac{a_0}{\tilde{\omega}}\left[\frac{\mathrm{d}\nabla_\mathrm{r}}{\mathrm{d}\tau}+(\nabla_\mathrm{r}-\nabla_\mathrm{a})\,\frac{2c}{r}\,h(\tau_\mathrm{d})\right]\,,\\ a_2&=-2a_0\;(\nabla_\mathrm{r}-\nabla_\mathrm{a})\,,\end{aligned} \tag{29a}$$

where

$$a_0=\frac{(\gamma-1)}{16\tilde{\omega}\tau_\mathrm{t}}\,\frac{g(1-\Delta_\mathrm{c})}{c\,\nabla_\mathrm{a}}\,. \tag{29b}$$

To facilitate the comparison between different models and expressions, we shall also consider the amplitude $A(\omega,\Delta)$ evaluated at a fiducial frequency and degree. Following MCDT, we define

$$\begin{aligned}A_{2.5}\equiv A(\tilde{\omega},\Delta=0)&=\left(a_1^2+a_2^2\right)^{1/2}\\ &=\frac{(\gamma-1)}{16\tilde{\omega}\tau_\mathrm{t}}\,\frac{g(1-\Delta_\mathrm{c})}{c\,\nabla_\mathrm{a}}\left\{4\,(\nabla_\mathrm{r}-\nabla_\mathrm{a})^2\right.\\ &\quad\left.+\frac{1}{\tilde{\omega}^2}\left[\frac{\mathrm{d}\nabla_\mathrm{r}}{\mathrm{d}\tau}+(\nabla_\mathrm{r}-\nabla_\mathrm{a})\,\frac{2c}{r}\,h(\tau_\mathrm{d})\right]^2\right\}^{1/2}\,.\end{aligned} \tag{30}$$

This gives the dependence of the amplitude $A_{2.5}$ on the acoustic position τ_d of the transition, and so also the implicit dependence on the acoustic extent $\tau_\mathrm{d}-\tau_\mathrm{c}$ of the overshoot region.

To study the actual variation of a_1, a_2 and $A_{2.5}$ with the extent of the overshoot region we need to know how the different functions of solar structure in equations (29a), (29b) and (30) vary when τ_d and τ_c are varied. Strictly speaking these expressions should be evaluated at the point τ_d of the sharp feature in the model. However, to get some feel for how the amplitudes would vary with the actual extent of overshoot we have taken two models, one without and one with overshoot, and have plotted the right-hand sides of equations (29a) and (30), evaluated at r, against $(r_\mathrm{c}-r)/H_p$, where r_c is the value of r at the edge of the unstable region and H_p is the pressure scale height. The results are shown in Fig. 1. As expected a_1 decreases from the value it has at the Schwarzschild boundary while a_2 increases from zero there. The cross-over between these two contributions gives rise to a shallow minimum in $A_{2.5}$ at modest overshoot distance.

If the method proposed by RV is used to obtain these expressions the result is approximately the same, for $l=0$. The application of their method to the signal in the frequencies is discussed in appendix B of MCDT. In Appendix C we use it to calculate the expressions (C6), (C7) for the oscillatory signal. These are quite similar to equation (24) (with $l=0$) together with expressions (29a) and (29b). The main advantage of the variational principle is that it also gives the dependence on the degree l. The additional contribution from Δ_c in equation (29b) has some effect for τ_d close to τ_c. The correction term in a_1 arising from $\nabla_\mathrm{r}-\nabla_\mathrm{a}$ also differs, but the difference is of little importance since the contribution of this term is small.

Rather than the expression (C6), RV present a simplified analysis which uses approximate dependences of the opacity on density and temperature at the base of the convection zone. The result is

$$\begin{aligned}A_\mathrm{RV}(\tilde{\omega})&=\frac{g}{12\tau_\mathrm{t}\tilde{\omega}\,c}\\ &\times\left[\left(\frac{g}{12\tilde{\omega}\,c}\right)^2\left(17-\frac{35}{\epsilon}+\frac{33}{\epsilon^2}\right)^2+\left(1-\frac{1}{\epsilon}\right)^2\right]^{1/2}\,,\end{aligned} \tag{31a}$$

with

$$\epsilon=\left(1+\frac{2}{5}\,\frac{r_\mathrm{c}-r_\mathrm{d}}{H_p}\right)^{15/4}\,. \tag{31b}$$

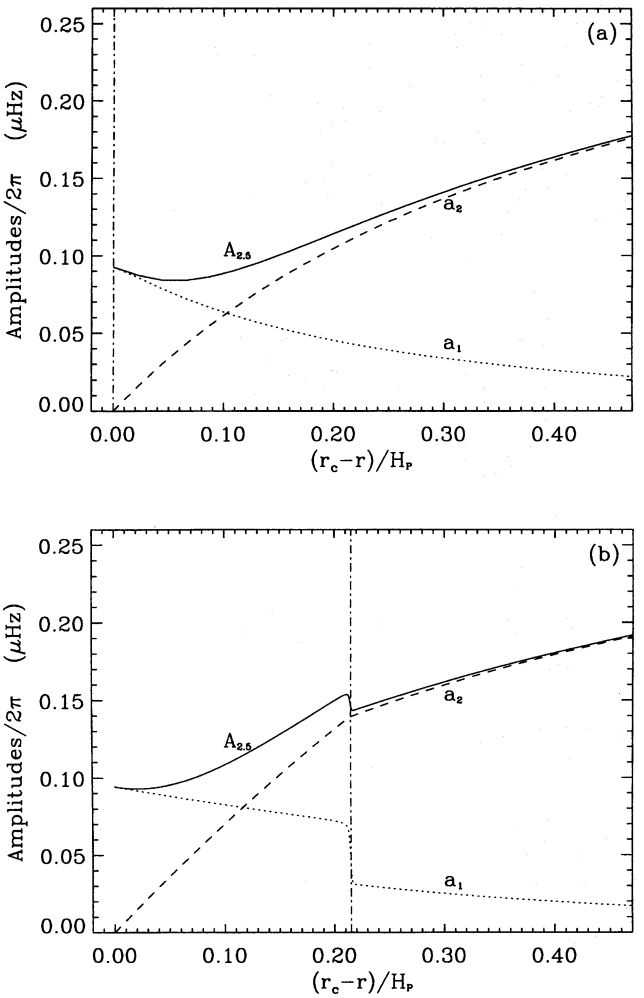

Figure 1. (a) Plot of the amplitude $A_{2.5}$ (continuous line) and the components a_1 (dotted line) and a_2 (dashed line) for an evolved solar model which has no overshoot (model Z_0 – see Table 1). (b) As (a) but for a model with overshoot (model Z_5 – see Table 1). The extent of the overshoot layer in this model is $0.215H_p$ (H_p being the pressure scale height). The dash-dotted lines indicate the point corresponding to $r=r_d$ for each model.

Here r_c and r_d are the radial positions corresponding to τ_c and τ_d, respectively.

5 SOLAR MODELS WITH OVERSHOOT

Static solar models with different extents of the overshoot layer at the base of the convection zone are considered. The models were calculated essentially as described by Christensen-Dalsgaard, Proffitt & Thompson (1993). The temperature gradient in the overshoot region was determined as described by MCDT, with each model having a different value of the parameter $\mathscr{D}$ which controls the extent of the region. Table 1 gives a list of the characteristics of these models.

From the p-mode frequencies of these models we have determined the parameters $(a_1, a_2, \bar{\tau}_d, \bar{\gamma}_d, \phi_0, \Delta_d)$ using the least-squares method described by MCDT (now also including Δ_d). The actual function fitted is given in equation (27). The set of modes used have degree l between 5 and 20 and frequencies smaller than 3500 μHz. These correspond to the same set of modes as used by MCDT to calibrate the solar values. This choice of mode set ensures that all our modes penetrate beneath the bottom of the convection zone, and excludes modes of very low degree or of high frequency which tend to have large observational errors.

Table 1. Characteristics of the models considered. The radial position r_c corresponds to the point where the radiative gradient equals the adiabatic gradient, while r_d is the position where the stratification changes from being almost adiabatic to being radiative. The solar radius is R.

Model	$\frac{r_c}{R}$	$\frac{r_d}{R}$	$\frac{r_c-r_d}{R}$	$\frac{r_c-r_d}{H_p}$
Z_0	0.72876	0.72876	0.00000	0.00000
Z_1	0.72871	0.72569	0.00302	0.03841
Z_2	0.72866	0.72246	0.00620	0.07886
Z_3	0.72857	0.71900	0.00957	0.12158
Z_4	0.72843	0.71529	0.01314	0.16693
Z_5	0.72823	0.71128	0.01695	0.21517
Z_6	0.72795	0.70692	0.02103	0.26683
Z_7	0.72759	0.70215	0.02544	0.32242
Z_8	0.72711	0.69690	0.03022	0.38256
Z_9	0.72650	0.69104	0.03546	0.44814

The results obtained from the fit are given in Table 2. As expected, the amplitude increases with the extent of the overshoot layer. The table also shows the results of fitting the solar data compiled by Libbrecht, Woodard & Kaufman (1990), using the same set of modes as for the models.

Fig. 2 compares the amplitude $A_{2.5}$ from the fit with the function obtained from the models by using expression (30). The results of the fit if we neglect the contribution from Δ are also shown. As argued by MCDT, the effect on $A_{2.5}$ of neglecting Δ is very small. As seen by comparing Table 2 with table 2 of MCDT, there is a more significant effect on the value of $\bar{\gamma}_d$: this is natural, given that $\bar{\gamma}_d$ determines the dependence on degree of the argument of the signal (cf. equation 25).

Comparison of the values of the amplitude predicted by equation (30) with the ones found by the fitting shows good agreement for overshooting distances larger than $0.1H_p$. However, for small overshoot distances the fit seems to give systematically smaller values. We return to this point in Section 7.

Fig. 2 also provides a comparison between equation (31a) obtained by RV, and the results found here from the variational principle and the fit to the signal in the frequencies. As shown, there is a systematic difference between the two theoretical predictions, although they have essentially the same shape. In particular, they both display the local minimum in the amplitude at small overshoot distance, first noted by RV and already indicated by the results shown in Fig. 1. It is interesting that the fit does not show such a minimum, although there is a noticeable departure from linearity at small r_c-r_d.

Results of applying the fitting procedure to the solar data are shown in Fig. 3. To estimate the effect of observational errors we have used 100 error realizations for the frequencies of model Z_2, with normally distributed errors added to the frequencies. The standard deviation for each mode was the quoted observational error in the data compiled by Libbrecht et al. (1990).

Table 2. Parameters obtained by fitting the frequency data with the expression of the signal as given in equation (27). The least-squares method used is described by MCDT. The acoustic depth is in seconds while $\bar{\gamma}_d$ and the amplitudes are in μHz. The parameters obtained for the solar data given by Libbrecht et al. (1990) are listed in the last row.

Model	$\bar{\tau}_d$	$\frac{\bar{\gamma}_d}{2\pi}$	ϕ_0	$\frac{A_{2.5}}{2\pi}$	Δ_d
Z_0	2260.4	11.5	1.28	0.0747	0.31
Z_1	2262.8	11.6	1.25	0.0789	0.31
Z_2	2268.0	12.2	1.19	0.0855	0.33
Z_3	2281.9	12.2	1.08	0.1049	0.31
Z_4	2293.3	12.8	0.98	0.1200	0.32
Z_5	2311.3	13.1	0.88	0.1435	0.30
Z_6	2328.4	13.7	0.78	0.1666	0.30
Z_7	2347.1	14.4	0.69	0.1916	0.30
Z_8	2367.4	14.9	0.61	0.2177	0.29
Z_9	2384.9	16.0	0.53	0.2433	0.30
Sun	2336.5	13.0	0.64	0.0853	0.29

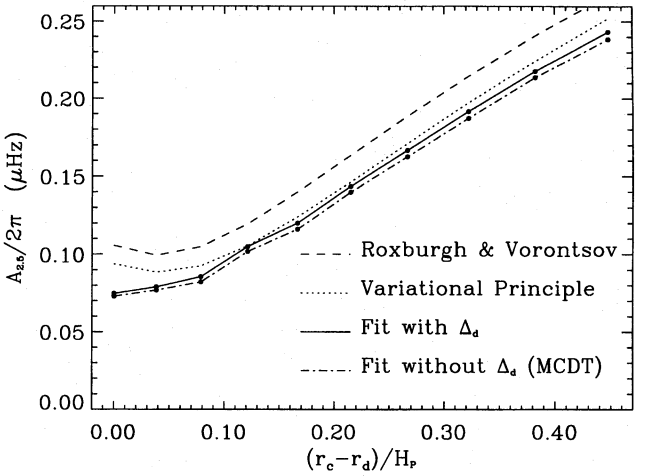

Figure 2. Plot of the amplitude $A_{2.5}$ for models Z_{0-9}. The continuous line corresponds to the values given by the fit if the dependence of the amplitude on the mode degree is considered. These are the values given in Table 2. The dot-dashed line corresponds to the fit for Δ_d=0, i.e., the expressions used by MCDT. The theoretical values as given from expression (30) are also plotted (dotted line) for all models. Finally, the dashed line shows the amplitude A_{RV} obtained from equation (31a) and corresponding to the results of Roxburgh & Vorontsov (1994).

6 EFFECTS OF A GRADUAL TRANSITION

We have so far assumed that there is an abrupt transition from the adiabatic to the radiative temperature gradient, in the case of overshooting leading to a discontinuity in ∇ at the point $r=r_d$ where the transition to the radiative gradient occurs. To illustrate the effects of relaxing this assumption, we have constructed models with the following structure for the overshoot region: from the boundary r_c of the unstable region to a point $r=r_a$ the stratification is assumed to be almost adiabatic, whereas between r_a and the bottom r_d of the overshoot region there is a smooth subadiabatic transition to radiative stratification.

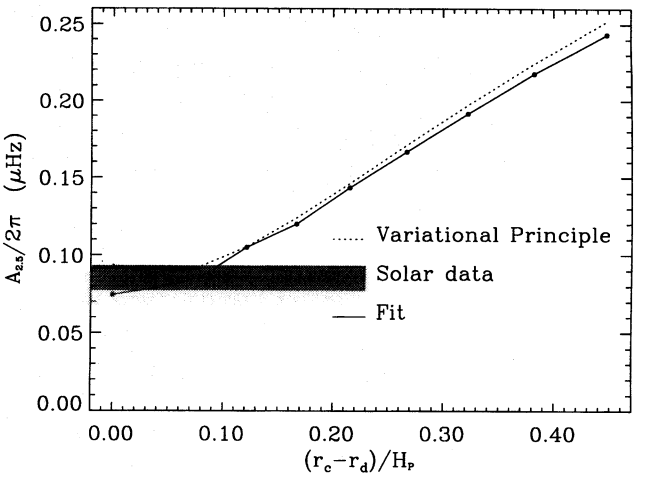

Figure 3. Plot of the amplitude $A_{2.5}$ for the fit (continuous line) and the expression from the variational analysis (dotted line) for all models Z_{0-9}. The result for the solar data (see Table 2) is also plotted as the shaded area which indicates the error as determined from 100 error realizations for model Z_2.

The stratification in some models of this nature, and the resulting fitted amplitudes, are illustrated in Fig. 4. In panel (a) the gradient in the overshoot region is shown for three such models (described below). For comparison, we also show the gradient in models Z_0 and Z_5 considered before: the former is a standard model with no overshoot, the gradient changing from the adiabatic to the radiative value at the instability limit, whereas the latter is an overshoot model with a sharp transition. The three new models are Z_a, Z_b and Z_c, which have a smoother transition from the adiabatic to the radiative value of the gradient in the overshoot region. For Z_a and Z_b there is no adiabatic stratification in the overshoot region, the models differing only in the extent of overshoot and hence of the smooth transition, while in Z_c half the overshoot region is adiabatically stratified, while the other half is the transition region. In panel (b) each model is indicated by a horizontal line at the amplitude obtained from the fit: the left-hand end corresponds to the depth r_a where the adiabatic stratification imposed by the overshoot ends, and the right-hand end corresponds to the point r_d where the stratification finally becomes radiative. Interestingly, even though the gradients in models $Z_a - Z_c$ are smooth, the transition gives rise to a larger maximum value of $|d\nabla/d\tau|$ than for the non-overshoot model; thus, on the scale of the modes the behaviour mimics that of an overshoot model, causing a modest increase in the amplitudes. The fitted amplitudes for the smooth models can be converted to a distance scale by calibrating against the fitted amplitudes of models with sharp overshoot regions. The inferred effective extent of overshoot for the smooth models is greater than the extent of the exactly adiabatic region (filled circles) but less than the distance from the base of the convectively unstable region to the point where the stratification becomes radiative (open circles). Roughly speaking, one may say that the fitted amplitude is an indicator of the extent of the almost adiabatic extension of the convection zone.

7 DISCUSSION

Our analysis is based upon the assumption that the transition from the convective region and overshoot layer to the radiative

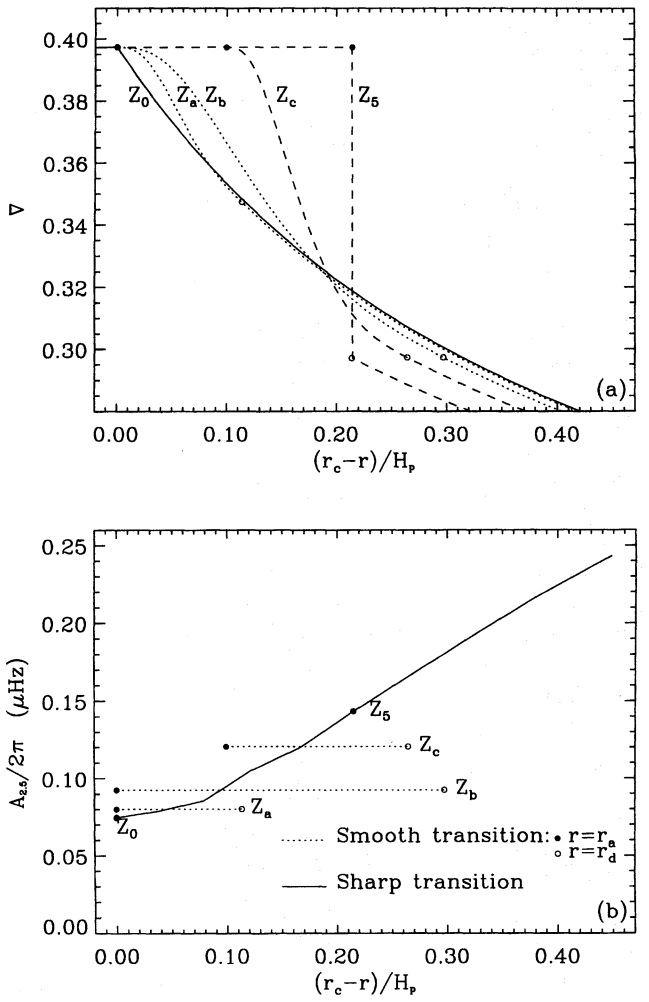

Figure 4. (a) Temperature gradient ∇ below the convection zone for five models (see the text), plotted against the distance r_c-r beneath the limit of the unstable region, in units of the pressure scale height H_p. (b) Plot of amplitude versus penetration distance for the overshoot models $Z_0 - Z_9$ (continuous line) and the new models Z_a, Z_b, Z_c. For these models we represent as a dotted line the region between the point (filled circle) where the region starts deviating from the adiabatic gradient and the point (open circle) where the gradient is finally radiative.

interior beneath takes place over a distance much shorter than the wavelength of the modes. This is indeed consistent with theoretical predictions that the extent of the transition region is of the order of 1 km (Zahn 1991). It is the abruptness of the transition that allows us to model its effect in terms of discontinuities of the derivatives of the sound speed.

A sharp transition in the solar structure gives rise to a quasi-periodic signal in the p-mode frequencies. In this paper we have derived a theoretical expression for the amplitude of this signal, by extending the application of the variational principle laid out by MCDT. The theory is in very good agreement with the amplitudes obtained by fitting frequencies of solar models, for overshoot distances larger than $0.1H_p$. For small overshoot distances the fit gives systematically smaller values than the ones predicted by expression (30). We note that, like ours, the results of Basu et al. (1994) show no evidence for the fitted amplitude being non-monotonic, even though Basu et al. similarly consider overshoot models with ℓ_s as small as $0.1H_p$. Since the theoretical amplitude is approximately the same for $\ell_s=r_c-r_d$ in the range from zero to $0.1\,H_p$, there seems to be no reason why fitting the signal should be more problematic for values close to zero than at about $0.1\,H_p$. We suspect, therefore, that the discrepancy between the fitted and predicted amplitudes for small ℓ_s is more probably associated with the incompleteness of the theoretical expressions than the incapacity of the fitting method. When there is little overshoot, the contribution from a_1 dominates; so it seems likely that the problem is associated with this coefficient.

The signal associated with the near-discontinuity of the third derivative is proportional to the derivative of the radiative gradient (and so to the derivative of the opacity at the base of the convection zone), while the signal associated with the near-discontinuity of the second derivative, which is present only if there is convective overshoot, is proportional to the difference between the radiative and adiabatic gradients at the point where the transition occurs. Our expression for the amplitude of the periodic signal gives values close to the predictions obtained with the simplified expression given by RV. They use a power law for the opacity to write the terms that appear as the radiative gradient or its derivative in our expression. As shown in Appendix C, their method does give almost the same expression when used together with our analysis. The main advantage of using the variational principle is that correction terms of about 10 per cent in magnitude can be included, together with the dependence of the amplitude on the degree of the modes. These two effects can account for up to 20 per cent of the amplitude associated with the term in the third derivative of the sound speed.

Under the assumption that the transition is sharp, MCDT (and similarly Basu et al. 1994) used solar data to infer that the extent of any overshoot region is much less than one pressure scale height. However, Roxburgh & Vorontsov (1994) found that the amplitude of the signal in the p-mode frequencies is not a monotonic function of the extent ℓ_s of the overshoot layer, when ℓ_s is small. Since MCDT's calibration interpolated between a model without overshoot and a model with an overshoot layer roughly $0.2\,H_p$ deep (which is rather greater than the inferred upper bound on the Sun's overshoot layer), we have considered it worthwhile to perform the calibration once more, using more models with small overshoot layers. Table 2 and Fig. 3 show how the amplitude obtained from fitting to solar data compares with the amplitudes from the models. Clearly the basic result obtained previously, that such a layer has to be small, is confirmed. A large overshoot layer (of the order of $0.2\,H_p$, say) would give rise to a much larger amplitude than we detect in solar data, even allowing for the non-monotonic behaviour highlighted by RV. However, because MCDT extrapolated linearly and the amplitude varies rather non-linearly for small overshoot layers, our published upper limit of $0.07\,H_p$ should be slightly increased, as can be judged from Fig. 3.

We stress again that the fundamental point upon which such a result is based is the assumption that the overshoot region is nearly adiabatically stratified with the transition to the radiative interior occurring over a very short length. If this is not the case, then the above conclusions must be modified. In Section 6 we investigated models in which the transition from nearly adiabatic stratification to the substantially subadiabatic stratification of the radiative interior takes place

over an extended region, though the transition still takes place within a fraction of one wavelength. In this case we found that the fitted amplitude, when calibrated against the amplitudes from models with a sharp transition, is a reasonable indicator of the radius at which the stratification begins to deviate from being adiabatic, but not of the point where the overshoot region finally peters out and the temperature gradient becomes radiative. The extended transition region in our models could represent a subadiabatic overshoot region in the Sun, extending beneath the adiabatic fraction of the overshoot layer, where the convective velocity field is non-zero but has only a weak effect on the thermodynamics of the layer. Hence a more precise interpretation of our present result, and similar published results, is that any adiabatically stratified overshoot region beneath the Sun's convective envelope cannot be more than a small fraction of a pressure scale height deep. We do not rule out a substantially deeper subadiabatic overshoot region in which weak mixing takes place.

ACKNOWLEDGMENTS

During part of this work MJPFGM was co-supported by grant BD-1274/91-RM from *Programa CIÊNCIA - JNICT*/Portugal. This work was supported in part by the UK Particle Physics and Astronomy Research Council, and by the Danish National Research Foundation through its establishment of the Theoretical Astrophysics Center.

REFERENCES

Basu S., Antia H.M., Narasimha D., 1994, MNRAS, 267, 209
Christensen-Dalsgaard J., Proffitt C.R., Thompson M.J., 1993, ApJ, 403, L75
Libbrecht K.G., Woodard M.F., Kaufman J.M., 1990, ApJS, 74, 1129
Monteiro M.J.P.F.G., Christensen-Dalsgaard J., Thompson M.J., 1994, A&A, 283, 247 (MCDT)
Roxburgh I.W., Vorontsov S.V., 1994, MNRAS, 268, 880 (RV)
Zahn J.-P., 1991, A&A, 252, 179

APPENDIX A: DERIVATIVES OF THE SOUND SPEED

The objective of this appendix is to write the derivatives of the sound speed as functions of the temperature gradient and its derivatives. From equation (1) we obtain the first derivative of the squared sound speed, with respect to acoustic depth τ, as

$$\frac{\mathrm{d}\log c^2}{\mathrm{d}\tau} = \frac{\mathrm{d}\log \Gamma_1}{\mathrm{d}\tau} + \frac{\mathrm{d}\log p}{\mathrm{d}\tau} - \frac{\mathrm{d}\log \rho}{\mathrm{d}\tau} . \tag{A1}$$

The derivative of the density can be eliminated by means of a thermodynamic relation, assuming constant abundances:

$$\frac{\mathrm{d}\log \rho}{\mathrm{d}\tau} = \frac{1-\chi_T \nabla}{\chi_\rho} \frac{\mathrm{d}\log p}{\mathrm{d}\tau} , \tag{A2}$$

where

$$\chi_T = \left(\frac{\partial \log p}{\partial \log T}\right)_\rho = \frac{\gamma-1}{\gamma} \frac{1}{\nabla_a}$$
$$\chi_\rho = \left(\frac{\partial \log p}{\partial \log \rho}\right)_T = \frac{\Gamma_1}{\gamma} \tag{A3}$$
$$\nabla = \frac{\mathrm{d}\log T}{\mathrm{d}\log p} .$$

Thus

$$\frac{\mathrm{d}\log \rho}{\mathrm{d}\tau} = \frac{\gamma}{\Gamma_1} \left(1 - \frac{\gamma-1}{\gamma} \frac{\nabla}{\nabla_a}\right) \frac{\mathrm{d}\log p}{\mathrm{d}\tau} , \tag{A4}$$

so that, finally,

$$\frac{\mathrm{d}\log c^2}{\mathrm{d}\tau} = \frac{\mathrm{d}\log \Gamma_1}{\mathrm{d}\tau} + \frac{\mathrm{d}\log p}{\mathrm{d}\tau} \left[1 - \frac{\gamma}{\Gamma_1}\left(1 - \frac{\gamma-1}{\gamma} \frac{\nabla}{\nabla_a}\right)\right] . \tag{A5}$$

In terms of acoustic depth the hydrostatic equation is

$$\frac{\mathrm{d}\log p}{\mathrm{d}\tau} = \frac{g\Gamma_1}{c} . \tag{A6}$$

After substitution, we are left with

$$\frac{\mathrm{d}\log c^2}{\mathrm{d}\tau} = \frac{\mathrm{d}\log \Gamma_1}{\mathrm{d}\tau} + \frac{g}{c} \left[(\Gamma_1-\gamma) + (\gamma-1) \frac{\nabla}{\nabla_a}\right] . \tag{A7}$$

Given the assumption of constant abundances this equation is general. However, since we want to apply it to the region around the base of the convection zone, we shall further assume that

$$\frac{\mathrm{d}\Gamma_1}{\mathrm{d}\tau} = 0 , \quad \frac{\mathrm{d}\gamma}{\mathrm{d}\tau} = 0 \quad \text{and} \quad \frac{\mathrm{d}\nabla_a}{\mathrm{d}\tau} = 0 . \tag{A8}$$

These are a very good approximation to the actual physics of the region since there the gas is fully ionized. As a result we obtain

$$\frac{\mathrm{d}c^2}{\mathrm{d}\tau} = gc\, y , \tag{A9}$$

where we introduced

$$y(\tau) = (\Gamma_1-1) + (\gamma-1) \frac{\nabla-\nabla_a}{\nabla_a} . \tag{A10}$$

Note that with assumptions (A8) this function is just $y=y(\nabla)$, since all other terms are constant.

The second derivative is now obtained by differentiating relation (A9), giving

$$\frac{\mathrm{d}^2 c^2}{\mathrm{d}\tau^2} = y \frac{\mathrm{d}(gc)}{\mathrm{d}\tau} + gc \frac{\mathrm{d}y}{\mathrm{d}\tau} ; \tag{A11}$$

using

$$\frac{\mathrm{d}g}{\mathrm{d}\tau} = -c\left(4\pi G\rho - \frac{2g}{r}\right) , \tag{A12}$$

we obtain

$$\frac{\mathrm{d}^2 c^2}{\mathrm{d}\tau^2} = -c^2\left(4\pi G\rho - \frac{2g}{r}\right) y + \frac{g^2}{2} y^2 + gc \frac{\mathrm{d}y}{\mathrm{d}\tau} . \tag{A13}$$

To calculate the third derivative we differentiate this equation once more to get

$$\frac{\mathrm{d}^3 c^2}{\mathrm{d}\tau^3} = \left[2 \frac{\mathrm{d}}{\mathrm{d}\tau}\left(\frac{gc^2}{r}\right) - 4\pi G \frac{\mathrm{d}(\rho c^2)}{\mathrm{d}\tau}\right] y + \frac{\mathrm{d}g^2}{\mathrm{d}\tau} \frac{y^2}{2} - \left[c^2\left(4\pi G\rho - \frac{2g}{r}\right) - \frac{\mathrm{d}(gc)}{\mathrm{d}\tau} - g^2 y\right] \frac{\mathrm{d}y}{\mathrm{d}\tau} + gc \frac{\mathrm{d}^2 y}{\mathrm{d}\tau^2} . \tag{A14}$$

Using

$$\frac{\mathrm{d}\log \rho}{\mathrm{d}\tau} = \frac{g}{c} (\Gamma_1 - y) , \tag{A15}$$

and (A12), equation (A14) becomes

$$\begin{aligned}\frac{\mathrm{d}^3c^2}{\mathrm{d}\tau^3} =& -gc\left[4\pi G\rho\left(\Gamma_1+\frac{2c^2}{rg}\right)-\frac{6c^2}{r^2}\right] y \\ & -gc\left(4\pi G\rho-\frac{4g}{r}\right) y^2 \\ & +2c^2\left(\frac{2g}{r}-4\pi G\rho+\frac{3g^2}{4c^2}\, y\right)\frac{\mathrm{d}y}{\mathrm{d}\tau}+gc\,\frac{\mathrm{d}^2y}{\mathrm{d}\tau^2}\,.\end{aligned} \tag{A16}$$

We may now obtain the final expressions for the sound speed and its derivatives. Substituting the expression for y, the first derivative becomes

$$\frac{\mathrm{d}c^2}{\mathrm{d}\tau} = gc\left[(\Gamma_1-1)+(\gamma-1)\,\frac{\nabla-\nabla_\mathrm{a}}{\nabla_\mathrm{a}}\right], \tag{A17}$$

while the second is, using again equation (A10),

$$\begin{aligned}\frac{\mathrm{d}^2c^2}{\mathrm{d}\tau^2} =& -c^2\left(4\pi G\rho-\frac{2g}{r}\right) \\ & \times\left[(\Gamma_1-1)+(\gamma-1)\,\frac{\nabla-\nabla_\mathrm{a}}{\nabla_\mathrm{a}}\right] \\ & +\frac{g^2}{2}\left[(\Gamma_1-1)+(\gamma-1)\,\frac{\nabla-\nabla_\mathrm{a}}{\nabla_\mathrm{a}}\right]^2 \\ & +\frac{gc(\gamma-1)}{\nabla_\mathrm{a}}\,\frac{\mathrm{d}}{\mathrm{d}\tau}(\nabla-\nabla_\mathrm{a})\,,\end{aligned} \tag{A18}$$

and the third is

$$\begin{aligned}\frac{\mathrm{d}^3c^2}{\mathrm{d}\tau^3} =& -gc\left[4\pi G\rho\left(\Gamma_1+\frac{2c^2}{rg}\right)-\frac{6c^2}{r^2}\right] \\ & \times\left[(\Gamma_1-1)+(\gamma-1)\,\frac{\nabla-\nabla_\mathrm{a}}{\nabla_\mathrm{a}}\right] \\ & -4gc\left(\pi G\rho-\frac{g}{r}\right)\left[(\Gamma_1-1)+(\gamma-1)\,\frac{\nabla-\nabla_\mathrm{a}}{\nabla_\mathrm{a}}\right]^2 \\ & +\frac{2gc^2(\gamma-1)}{\nabla_\mathrm{a}}\left\{\frac{2}{r}-\frac{4\pi G\rho}{g}+\frac{3g}{4c^2}\right. \\ & \left.\times\left[(\Gamma_1-1)+(\gamma-1)\,\frac{\nabla-\nabla_\mathrm{a}}{\nabla_\mathrm{a}}\right]\right\}\frac{\mathrm{d}}{\mathrm{d}\tau}(\nabla-\nabla_\mathrm{a}) \\ & +\frac{gc(\gamma-1)}{\nabla_\mathrm{a}}\,\frac{\mathrm{d}^2}{\mathrm{d}\tau^2}(\nabla-\nabla_\mathrm{a})\,.\end{aligned} \tag{A19}$$

These are of the form given in equations (2) – (4).

APPENDIX B: VARIATIONAL PRINCIPLE

We start from the expression for the periodic component of the frequency differences which is given by (see appendix A of MCDT)

$$\begin{aligned}\delta\omega \sim \frac{1}{4\omega^2\tau_\mathrm{t}}\int_{\tau_\mathrm{a}}^{\tau_\mathrm{b}}\Bigg[& -\frac{\sin(\Lambda)}{4\omega^2(1-\Delta)^{3/2}}\,\frac{\mathrm{d}^3\delta B_1}{\mathrm{d}\tau^3} \\ & -\frac{\cos(\Lambda)}{2\omega(1-\Delta)}\,\frac{\mathrm{d}^3}{\mathrm{d}\tau^3}(\delta B_0+\delta B_2) \\ & +\frac{\sin(\Lambda)}{(1-\Delta)^{1/2}}\,\frac{\mathrm{d}^3\delta B_3}{\mathrm{d}\tau^3}\Bigg]\,\mathrm{d}\tau\,,\end{aligned} \tag{B1}$$

where τ_t is the total acoustic depth of the Sun and the other variables are as defined in the main text. The interval of integration is such that the sound-speed difference and its derivatives are zero outside the region $\tau_\mathrm{a}\leqslant\tau\leqslant\tau_\mathrm{b}$.

The functions δB_i are (see MCDT)

$$\begin{aligned}\frac{\delta B_1}{\omega^2} &\sim \left[-\frac{1}{1-\Delta}+\frac{g_0}{\omega^2c_0}\,\frac{\mathrm{d}}{\mathrm{d}\tau}\log\left(\frac{g_0}{r_0^2}\right)+\mathcal{O}(\omega^{-4})\right]\frac{\delta c^2}{c_0^2}\,, \\ \frac{\delta B_0+\delta B_2}{\omega} &\sim \mathcal{O}(\omega^{-3})\;\;\frac{\delta c^2}{c_0^2}\,, \\ \delta B_3 &\sim -\frac{1}{2}\,\frac{\Delta}{(1-\Delta)^2}\;\;\frac{\delta c^2}{c_0^2}\,.\end{aligned} \tag{B2}$$

In writing these we have neglected already the contribution from $\delta(\Gamma_1 p)$, and used the fact that $\Delta\sim\mathcal{O}(\omega^{-2})$. The subscript '$_0$' represents the smooth model, defined such as to have no discontinuous derivatives, relative to which we consider the sound-speed differences.

The next step is to neglect terms of order $\mathcal{O}(\omega^{-3})$ or smaller in the integrand in equation (B1), leaving

$$\begin{aligned}\delta\omega \sim & -\frac{1}{16\omega^2\tau_\mathrm{t}}\int_{\tau_\mathrm{a}}^{\tau_\mathrm{b}}\frac{\sin(\Lambda)}{(1-\Delta)^{3/2}} \\ & \times\left\{\frac{\mathrm{d}^3}{\mathrm{d}\tau^3}\left[\left(-\frac{1}{1-\Delta}+\Delta_c\right)\frac{\delta c^2}{c_0^2}\right]\right. \\ & \left.+2(1-\Delta)\,\frac{\mathrm{d}^3}{\mathrm{d}\tau^3}\left[\frac{\Delta}{(1-\Delta)^2}\,\frac{\delta c^2}{c_0^2}\right]\right\}\mathrm{d}\tau\,,\end{aligned} \tag{B3}$$

where Δ_c was defined in equation (16). Now, we neglect second derivatives of the equilibrium quantities and take only the terms that are proportional to the second and third derivatives of the sound-speed difference, to obtain

$$\begin{aligned}\delta\omega \sim & -\frac{1}{16\omega^2\tau_\mathrm{t}}\int_{\tau_\mathrm{a}}^{\tau_\mathrm{b}}\frac{\sin(\Lambda)}{(1-\Delta)^{3/2}} \\ & \times\left[-\left(\frac{1-2\Delta}{1-\Delta}-\Delta_c\right)\frac{\mathrm{d}^3}{\mathrm{d}\tau^3}\left(\frac{\delta c^2}{c_0^2}\right)\right. \\ & \left.+\frac{6\Delta(1+2\Delta)}{(1-\Delta)^2}\,\frac{\mathrm{d}}{\mathrm{d}\tau}\log\left(\frac{c_0}{r_0}\right)\,\frac{\mathrm{d}^2}{\mathrm{d}\tau^2}\left(\frac{\delta c^2}{c_0^2}\right)\right]\mathrm{d}\tau.\end{aligned} \tag{B4}$$

Since at most the first derivative of the sound speed is discontinuous, the only terms that may contribute with a δ function are the second and third derivatives of the sound speed.

APPENDIX C: ROXBURGH & VORONTSOV METHOD

Here, we shall consider a different method to obtain the expressions for the signal from the one given in the main text. It corresponds to the method used by Roxburgh & Vorontsov (1994), but applied to the signal in the frequencies and not in the phase function.

We start by considering the acoustic potential for the oscillations, which is (see RV)

$$\begin{aligned}V^2(\tau) =& N^2+\frac{c^2}{4}\left(\frac{2}{r}+\frac{N^2}{g}-\frac{g}{c^2}-\frac{1}{2c^2}\,\frac{\mathrm{d}c^2}{\mathrm{d}r}\right)^2 \\ & -\frac{c}{2}\,\frac{\mathrm{d}}{\mathrm{d}r}\left[c\left(\frac{2}{r}+\frac{N^2}{g}-\frac{g}{c^2}-\frac{1}{2c^2}\,\frac{\mathrm{d}c^2}{\mathrm{d}r}\right)\right] \\ & -4\pi G\rho\,,\end{aligned} \tag{C1}$$

N being the Brünt–Vässäla frequency. Using again approxima-

tions (A8) and relations (8), (9), and (10) this can be written as

$$V^2(\tau) = \left(\frac{g\Gamma_1}{2c}\right)^2 + \frac{2g}{r}(\Gamma_1-2) + \frac{2c^2}{r^2} - 2\pi G\rho\Gamma_1 + \left(\pi G\rho - \frac{g}{2r} - \frac{g^2\Gamma_1}{2c^2}\right) \times \left[\Gamma_1-1+(\gamma-1)\frac{\nabla_r-\nabla_a}{\nabla_a} H(\tau-\tau_d)\right] + \frac{g^2}{16c^2}\left\{(\Gamma_1-1)^2+(\gamma-1)\frac{\nabla_r-\nabla_a}{\nabla_a} \times \left[2(\Gamma_1-1)+(\gamma-1)\frac{\nabla_r-\nabla_a}{\nabla_a}\right] H(\tau-\tau_d)\right\} - \frac{g}{4c}\left[(\gamma-1)\frac{\nabla_r-\nabla_a}{\nabla_a}\delta(\tau-\tau_d) + \frac{\gamma-1}{\nabla_a}\frac{d\nabla_r}{d\tau} H(\tau-\tau_d)\right]. \quad \text{(C2)}$$

Thus we obtain an expression of the form

$$V^2(\tau) = V_0^2(\tau) + A_H(\tau)\, H(\tau-\tau_d) + A_\delta(\tau)\,\delta(\tau-\tau_d), \quad \text{(C3)}$$

where

$$V_0^2(\tau) = \frac{g}{2r}(3\Gamma_1-7) + \frac{2c^2}{r^2} - \pi G\rho(\Gamma_1+1) - \frac{g^2}{16c^2}(\Gamma_1+1)(\Gamma_1-3),$$
$$A_H(\tau) = -\frac{g(\gamma-1)}{2r}\frac{\nabla_r-\nabla_a}{\nabla_a}\bar{h}(\tau) - \frac{g(\gamma-1)}{4c\nabla_a}\frac{d\nabla_r}{d\tau}, \quad \text{(C4)}$$
$$A_\delta(\tau) = -\frac{g(\gamma-1)}{4c\nabla_a}(\nabla_r-\nabla_a),$$

and the function $\bar{h}(\tau)$ is

$$\bar{h}(\tau) = 1 - \frac{4\pi G r\rho}{2g} + \frac{rg(\Gamma_1+3)}{4c^2} - \frac{3rg}{8c^2}(\gamma-1)\frac{\nabla_r-\nabla_a}{\nabla_a}. \quad \text{(C5)}$$

It follows that the periodic signal in the frequencies is given by (see RV and MCDT's appendix B)

$$\delta\omega = -\frac{A_H(\tau_d)}{4\omega\tau_t}\sin(\Lambda) + \frac{A_\delta(\tau_d)}{2\omega^2\tau_t}\cos(\Lambda) = a_1\left(\frac{\tilde{\omega}}{\omega}\right)^2\sin(\Lambda) + a_2\left(\frac{\tilde{\omega}}{\omega}\right)\cos(\Lambda) \quad \text{(C6)}$$

with the components given by

$$a_1 = \frac{a_0}{\tilde{\omega}}\left[\frac{d\nabla_r}{d\tau} + (\nabla_r-\nabla_a)\frac{2c}{r}\bar{h}(\tau_d)\right] \quad \text{(C7)}$$
$$a_2 = -2a_0(\nabla_r-\nabla_a)$$

where

$$a_0 = \frac{1}{16\tilde{\omega}\tau_t}\frac{g(\gamma-1)}{c\nabla_a}, \quad \text{(C8)}$$

and all quantities are evaluated at $\tau=\tau_d$. These correspond to the expressions found using the variational principle, the main difference being the fact that the variational principle also gives the dependence on the degree of the modes. The other differences are just small corrections such as the term in Δ_c or the, otherwise rather different, terms in h and $\bar{h}$.

This paper has been produced using the Royal Astronomical Society/Blackwell Science TEX macros.